Jour. Fac. Sci., Hokkaido Univ., Ser. VII (Geophysics), Vol. 11, No. 1, 249-264, 1998.

A Technique for Detecting Vortexes Using the Gradient of Doppler Velocity Data

Toshihiro Haneda* and Hiroshi Uyeda

Division of Earth and Planetary Sciences, Graduate School of Science, Hokkaido University, Sapporo 060-0810, Japan

(Received November 30, 1997)

Abstract

We applied the method of detecting gust fronts and shear lines to the detection of the vortex in order to develop a simple technique for automatically detecting vortexes with Doppler velocity data obtained from a single Doppler radar. We calculated the velocity gradient along the range directions and along the azimuthal directions. If we recognize the shear pattern from the Doppler velocity field, a vortex (its location of the center and horizontal extent) will be detected. The analyses are performed on the Doppler velocity data of the cyclonic and the anticyclonic vortex close to Chitose Airport, Hokkaido, Japan on 22 September 1988. Rotational orientation and size are calculated by the conventional method for the analyses of a vortex and compared with the analyses by the vortex detection method. The diameter of the cyclonic vortex near 2,500 m in height remained about 10 km. Since we applied the method of detecting gust fronts and shear lines to this technique, the vortex and gust front (shear line) are detected at the same time.

1. Introduction

Many studies on the vortex of mesocyclones and hurricanes with single Doppler radar have been carried out by Zrnic' et al. (1984), Wood (1994) and others. Development and improvement of the technique used in detecting vortexes (from ten to a few dozen kilometers in horizontal scale) with Doppler velocity data obtained from a single Doppler radar are essential for the recognition and prediction of cloud development and tornado formation. An algorithm to detect the vortex signature (esp., small and strong vortexes) in a cloud is necessary for short-time forecasts and aviation safety (e.g., the prevention of accidents).

We develop a simple technique to detect vortexes automatically with Doppler velocity data obtained from a single Doppler radar. This technique

* On leave from Japan Radio Co., Ltd., Mitaka Tokyo 181-8510, Japan.

applied the method of detecting gust fronts and shear lines (Uyeda and Zrnic', 1986, 1988) to the detection of vortex patterns in the case of anticyclonic and cyclonic vortexes. We think it possible to recognize cyclonic or anticyclonic vortex, and calculate the diameter of the vortex. Since we applied the method of gust front (shear line) detection to this technique, we think it also possible to detect both gust fronts (shear line) and vortexes at the same time in the actual routine of the operation.

2. New detection techniques

Figure 1 represents an outline of the technique used in detecting a vortex. When we calculate the velocity gradient ($\Delta Vr/\Delta r$) along range directions for an anticyclonic vortex existing in general wind, we will detect the shear of convergence (hereafter called the SRD: Shear of Range Direction) both on the right front side and the left back side looking from the radar. When we calculate the velocity gradient ($\Delta Vr/r\Delta\theta$) along azimuthal directions, we will detect the shear near the core region of the vortex (hereafter called the SAD: Shear of Azimuthal Direction). If we recognize a pattern in the Doppler velocity field in which SRD exists on the opposite side of SAD, a vortex (its location of the center and horizontal extent) will be detected. On the other hand, a cyclonic vortex will be detected as a pattern symmetrical to that of the anticyclonic vortex.

In the test analysis we used data of the range resolution of 250 m (64 km/256 range) and the azimuthal resolution of 0.7 degree (360 degree/512 sweep). A brief description of the detection of the shear is given as follows. For the extraction of the shear, five points average (after de-aliasing) radial (or azimuthal) velocity was used. The gradient of the range direction (g_r) and the gradient of the azimuthal direction (g_a) are defined as

$$g_r=(v_{n+2}-v_{n-2})/(r_{n+2}-r_{n-2})$$

$$g_a=(v_{n+2}-v_{n-2})/r_n(az_{n+2}-az_{n-2})$$

where v_n of g_r is a smoothed velocity corresponding to a range r_n between beginning (r_{n-2}) and ending (r_{n+2}) ranges. Similarly, v_n of g_a is a smoothed velocity corresponding to an azimuth az_n between beginning (az_{n-2}) and ending (az_{n+2}) azimuths. In order to choose the best threshold of the detection of SRD and SAD, the detection was tested with the values $\pm 2\times10^{-3}s^{-1}$, $\pm 3\times10^{-3}s^{-1}$, $\pm 4\times10^{-3}s^{-1}$ one after another. In results, the vortex pattern was detected the most clearly when the threshold was $\pm 2\times10^{-3}s^{-1}$. Therefore, in the present

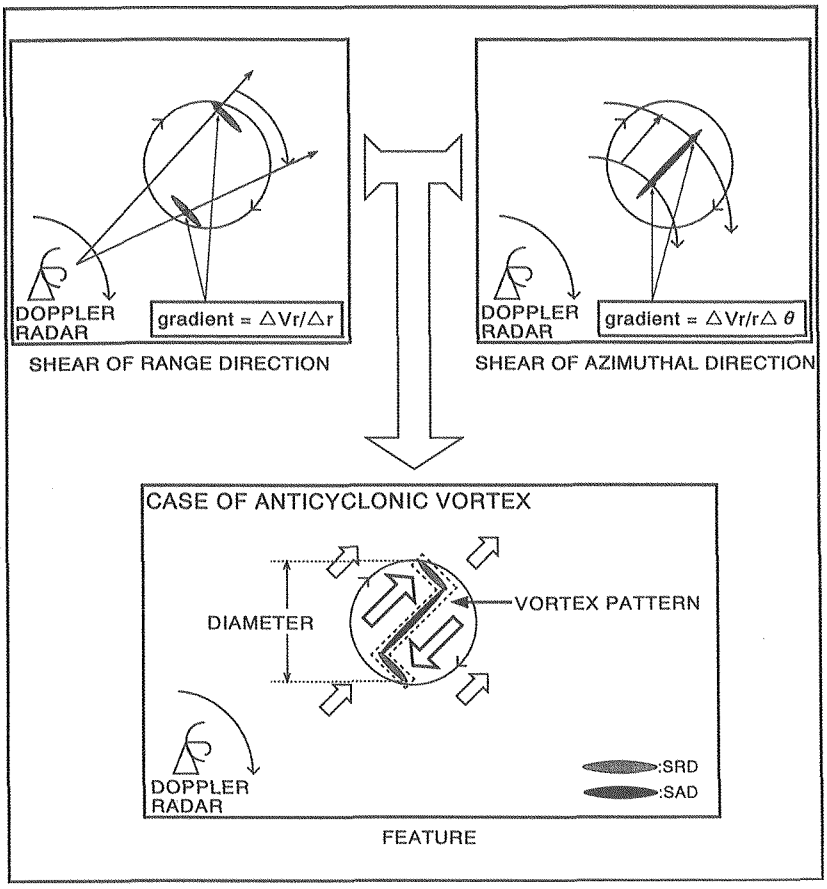

Fig. 1. Schematic illustration of the technique to detect a vortex.

study, we used the threshold of $\pm 2 \times 10^{-3} s^{-1}$ for the detection of SDR and SAD. In order to identify a vortex signature, the maximum gradient points of SRD and SAD were grouped into a vortex signature with the minimum radial distance of 1 km and an azimuthal separation of 2.1 degree (at the 30 km range, the distance is about 1.1 km).

3. Data

We used the Doppler velocity data of the cyclonic and the anticyclonic vortex close to Chitose Airport, Hokkaido, Japan on 22 September 1988 (Shirooka and Uyeda, 1991 ; Kobayashi et al., 1996). The data was collected by the

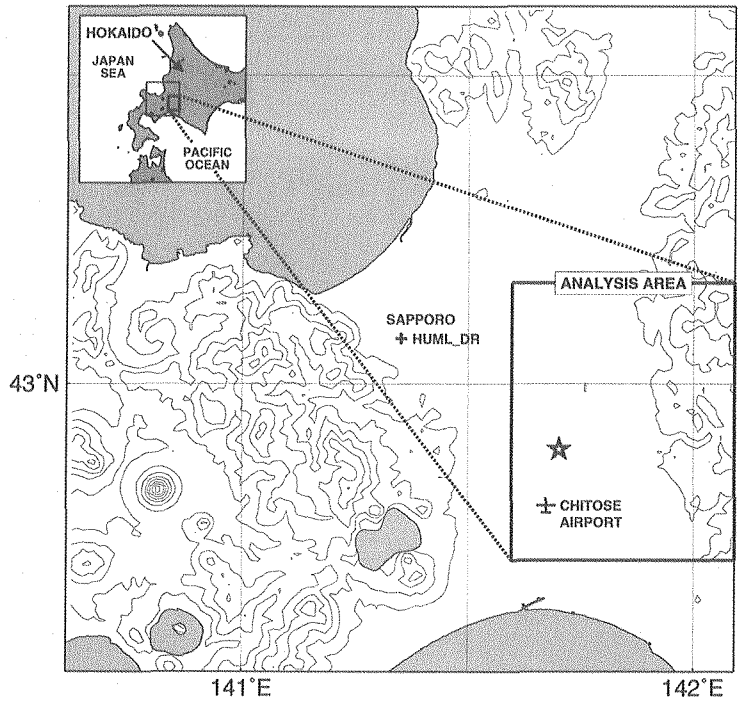

Fig. 2. Map of the analysis area. Topography shown with 200 m contour intervals. A star mark and a cross mark (HUML_DR) denote the locations of the tornado and the radar site respectively. Analyses were made for the rectangular area (analysis area).

Hokkaido University Meteorological Laboratory X-band Doppler radar (HUML_DR). The PPI data of three elevation angles (3°, 4° and 6°) at 10 minute intervals and that of RHI in the direction crossing the vortex were utilized for analyses.

In the analyses by Shirooka and Uyeda (1991), parent cyclonic circulations and tornado circulations were revealed from 1303JST to 1353JST, 22 September 1988. Here JST (Japan Standard Time) is 9 hours ahead of UTC. Before the time of the tornado development anticyclonic circulations were recognized on the display of Doppler velocity field about 15 km northeast of the tornado producing echo cell (Takahashi et al., 1991).

Figure 2 shows a map of the analysis area. A star mark denotes the location of the tornado. Doppler velocity data in the rectangular area (analysis area) was analyzed in detail.

4. Results

4.1 Vortex pattern

An example of vortex pattern detection is shown in Fig. 3. Points of the maximum radial gradient of radial velocity (open circle) and the maximum azimuthal gradient of radial velocity (solid circle) form the pattern of an anticyclonic vortex of SRD and SAD as shown in Fig. 1. The pattern coincides well with that of Fig. 1 except for the right front edge of SRD. The right front side has an echo-less region. Variations of radial velocities along R1 and R2 in Fig. 3 are shown in Fig. 4(a). Open circles denote the location of the maximum radial gradient of radial velocity. Figure 4(b) shows the azimuthal variation of radial velocity along A1 in Fig. 3. Solid circles denote the location of the maximum azimuthal gradient of radial velocity. These maximum gradient points form lines of SRD and SAD, and a vortex pattern. This example of vortex detection encourages us to use the method for the automatic detection of

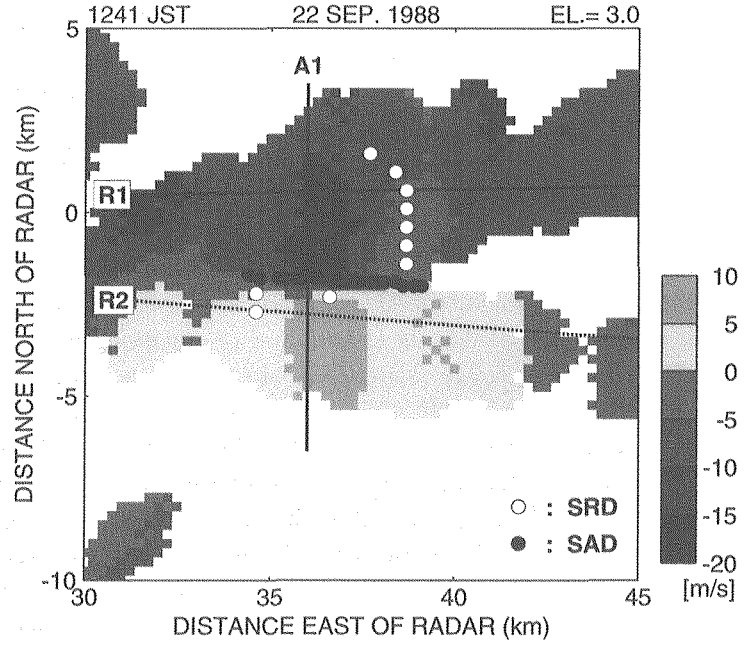

Fig. 3. Doppler velocity field and the detected vortex pattern at 1241JST, 22 September 1988. The elevation angle is 3.0°. Open circle indicates the location of the radial gradient of radial velocity along each range. Solid circle indicates the location of maximum azimuthal gradient of radial velocity. Here, negative in the velocity pattern denotes the velocity component away from the radar.

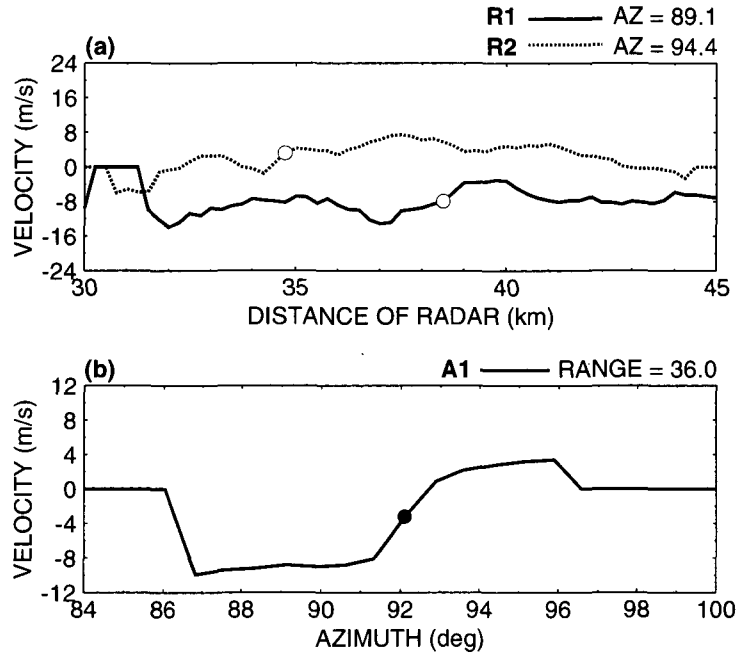

Fig. 4. Variations of radial velocities along (a) R1 and R2, and (b) A1 in Fig. 3. Open circles denote the locations of the maximum radial gradient of radial velocity. Solid circles denote the location of the maximum azimuthal gradient of radial velocity.

vortex signatures.

In the analyses by Shirooka and Uyeda (1991) and Kobayashi et al. (1996), cloud circulations were revealed at the elevation of 4.0° for the entire time of the parent cyclonic circulation, so we carried out detection of the vortex patterns for the data at the elevation of 4.0°. Figure 5 shows the detections of vortex patterns at the elevation angle of 4.0° (after the time of Fig. 3). These data were taken at 10 minute intervals. Anticyclonic vortex patterns are detected as shown in VORTEX_A1 in Fig. 5(a), A2 in (b), A3 in (c) and A4 in (d), and a cyclonic pattern in VORTEX_B1 in Fig. 5(d), B2 in (e), B3 in (f), B4 in (g) and B5 in (h). Here, points of SRD and SAD are shown by solid circles. The wind fields obtained with the TVAD method (Takahashi et al., 1991) are superposed in Fig. 5. The height of the vortex patterns detected were about 2,500 m. Six of nine vortex patterns analyzed were detected as clearly having the signature of a vortex.

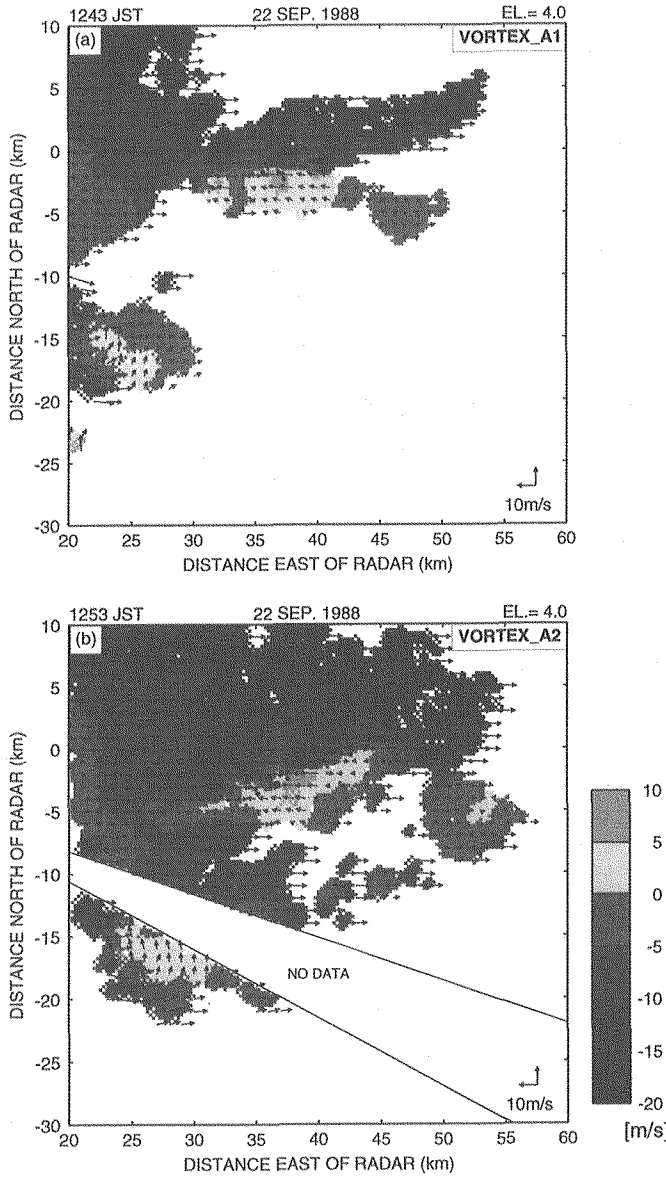

Fig. 5. Detection of vortex patterns after the time of Fig. 3. These data were taken at 10 minute intervals (1243JST to 1353JST), 22 September 1988. The elevation angle is 4.0°. VORTEX_A1 in (a), A2 in (b), A3 in (c) and A4 in (d) are anti-cyclonic vortexes and VORTEX_B1 in (d), B2 in (e), B3 in (f), B4 in (g) and B5 in (h) are a cyclonic vortex. Solid circles are points of SRD and SAD. The wind field with the TVAD method (Takahashi et al., 1991) are superposed. Velocity pattern is the same as Fig. 3.

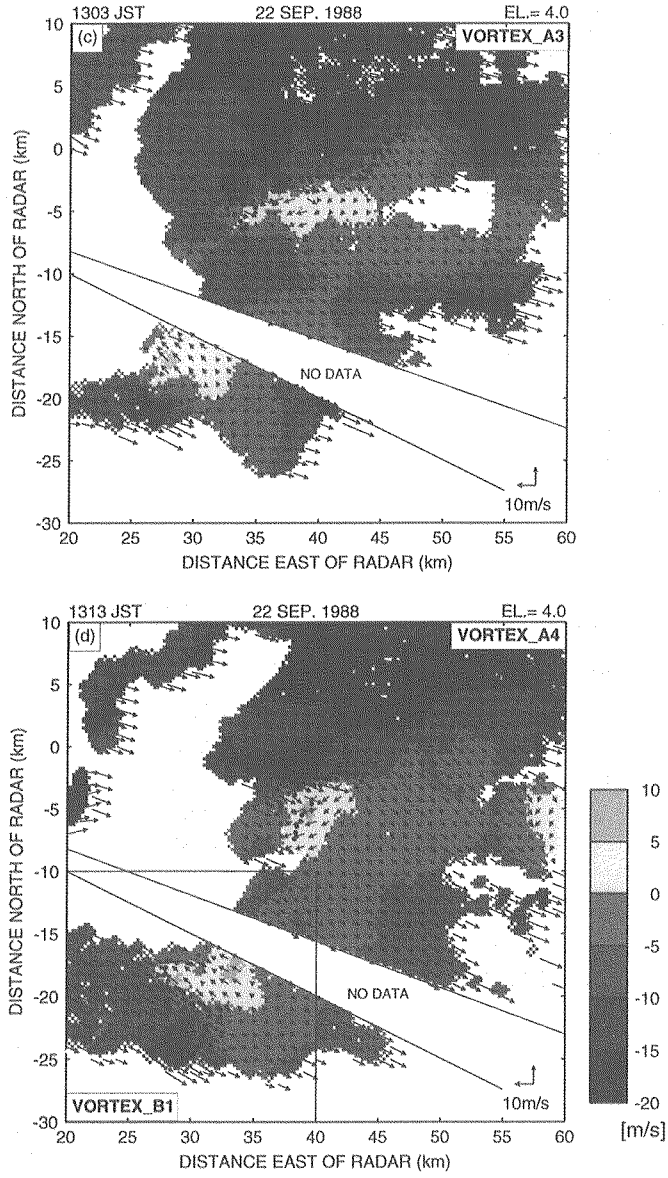

Fig. 5 (Continued)

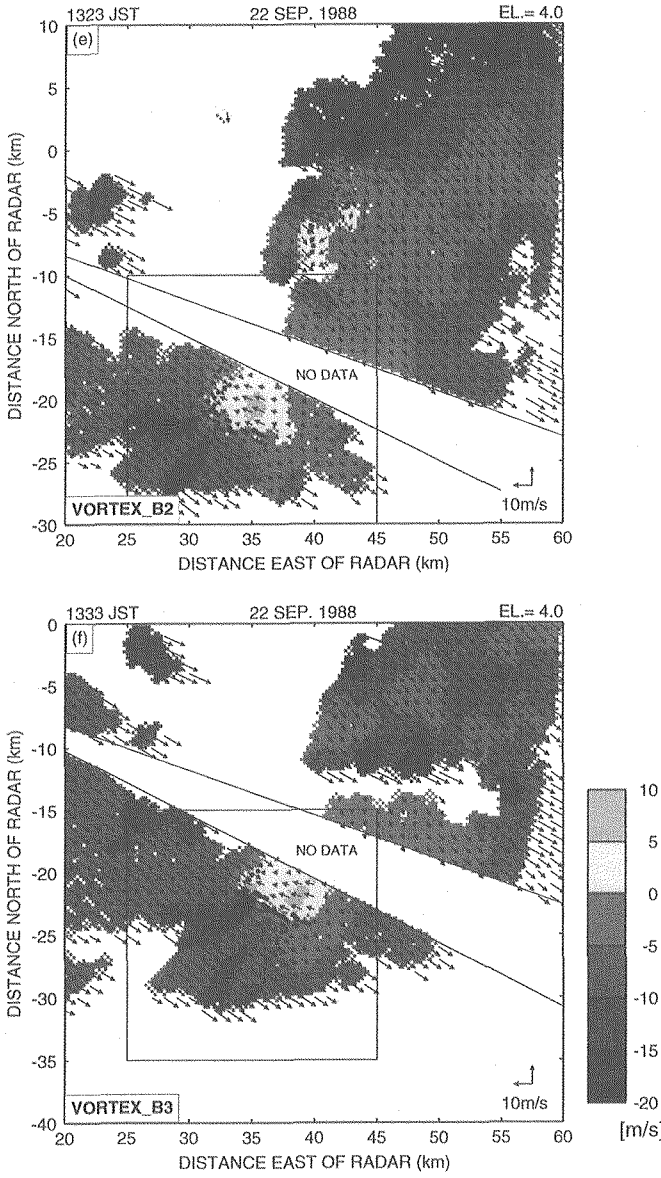

Fig. 5 (Continued)

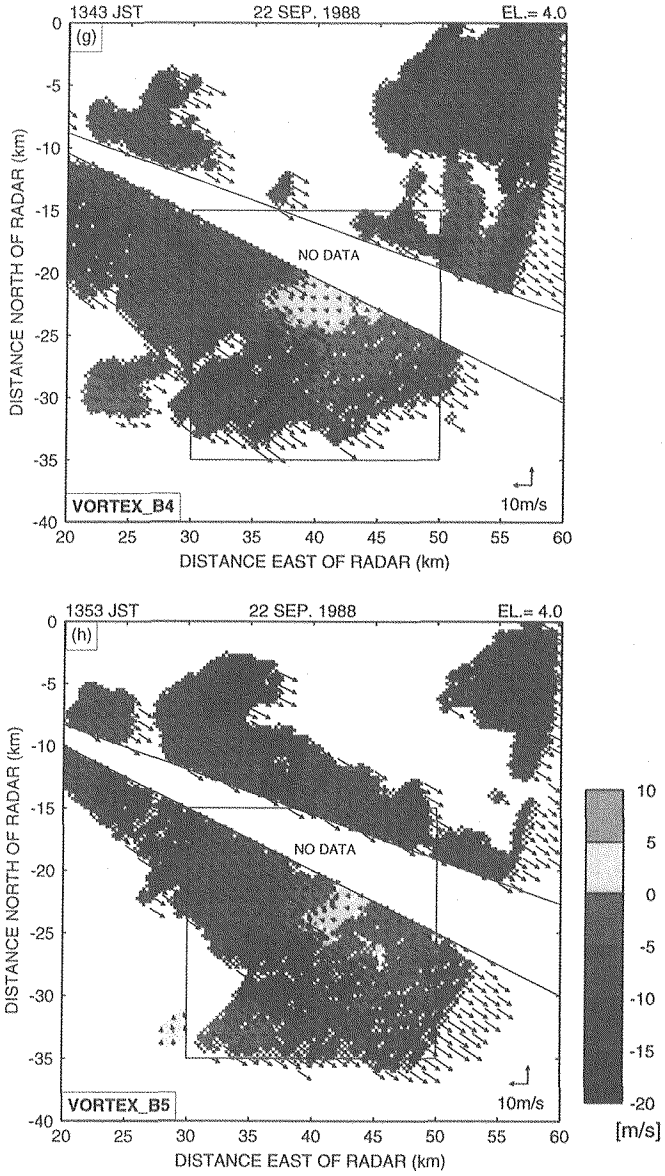

Fig. 5 (Continued)

4.2 Diameter of vortex

We compared the location and size of the vortex pattern estimated by the assumptions of the Rankine vortex (Wood and Brown, 1983), with those obtained by the present automated method because the cyclonic vortex kept a symmetric

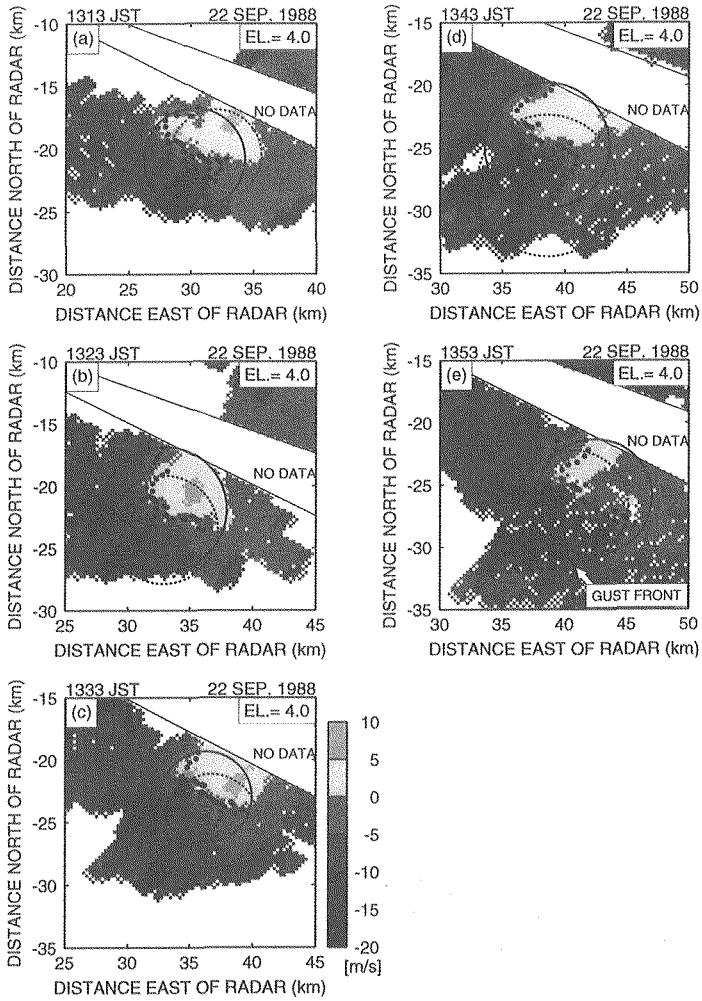

Fig. 6. Location and size of vortex pattern estimated by the assumption of the Rankine vortex (dashed circle) and that obtained by the present automated method (solid circle) from 1313JST to 1353JST, 22 September 1988. Velocity pattern is the same as Fig.3. Flames (a), (b), . . . , (e) correspond to box areas including VORTEX_B1, B2, . . . , B5 in Fig. 5 respectively.

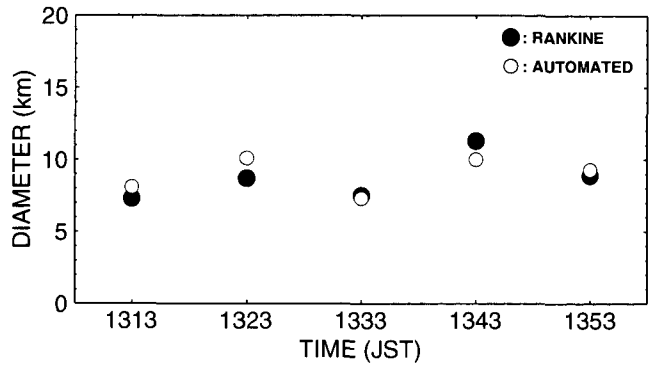

Fig. 7. Comparison of the diameters of vortex patterns estimated by the assumption of the Rankine vortex (●) with that obtained by the present method (○).

pattern. Figure 6(a) to (e) shows the location of the vortex pattern. The dashed circle denotes the location and size of the vortex pattern estimated by the assumption of the Rankine vortex. The solid circle denotes those obtained by the present automated method. These two corresponded well with each other while the vortex kept a symmetric pattern. In the case of Fig. 6(e), a gust front was detected at the same time.

We compared the diameters of cyclonic vortex patterns estimated by the assumptions of the Rankine vortex, with those obtained by the present automated method. Figure 7 shows the time variation of the diameters of the vortex pattern determined by the two methods. These also coincided well with each other.

5. Discussion

The new method proposed performed well in the detection of symmetric vortex patterns as shown in Fig. 3, VORTEX_A1 and VORTEX_B1 to B5 in Fig. 5. However, SRD was not well detected in VORTEX_A2 to A4 in Fig. 5. We studied the relation between the orientation of SAD (thick line) and the direction of the radar beam (open wide arrow) as shown in Fig. 8. The orientation of SAD is parallel to the radar beam in Fig. 8(a) and Fig. 8(e) to (h), but is tilting to the radar beam in the case of Fig. 8(b) to (d). We can consider that the form of the vortex is an ellipse, and this tilting of its long axis (SAD) to the radar beam is the reason why we failed to detect the vortex pattern in VORTEX_A2 to A4 in Fig. 5. We also consider that the vortex in VORTEX_A2 to A4 in Fig. 5 are the same as the pattern of TYPE T in Fig. 9, which is drawn referring to

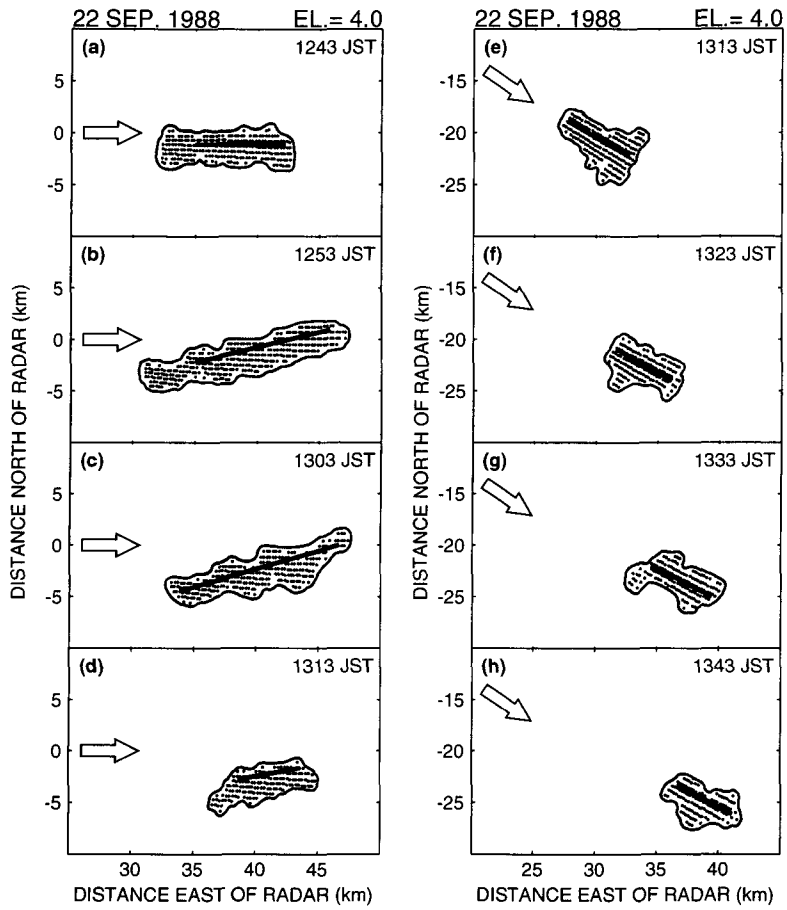

Fig. 8. Areas (enclosed by solid line) of the large azimuthal gradient ($>2.0\times10^{-3}s^{-1}$ for (a) to (d); $<-2.0\times10^{-3}s^{-1}$ for (e) to (h)) of radial velocity and the SAD (thick line) of the detected vortex pattern. Open wide arrow indicates the direction of the radar beam. (a), (b), (c) and (d) correspond to VORTEX_A1, A2, A3 and A4 (anticyclonic vortex) in Fig. 5 respectively. (e), (f), (g) and (h) correspond to VORTEX_B1, B2, B3 and B4 (cyclonic vortex) in Fig. 5 respectively.

Desrochers and Harris (1996). In the case of TYPE T, we detected the shear near the core region of the vortex by SRD and SAD. If we recognize SRD and SAD near the core region of the vortex at the same time, a ellipse vortex could be detected.

We compared the diameters and location of the center of vortex patterns estimated by the assumptions of the Rankine vortex with those obtained by the present automated method for the cyclonic vortex. Diameters corresponded

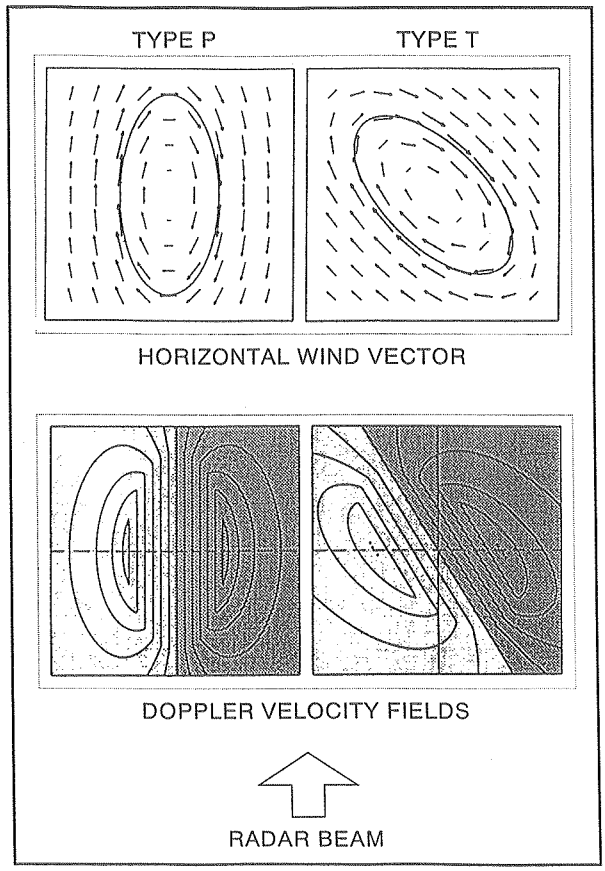

Fig. 9. Schematic illustration of the wind field and Doppler velocity pattern of the elliptical anticyclonic vortex. Shaded area indicates the Doppler velocity toward a radar and contour shows radial speed. Type P and Type T are elliptical anticyclonic vortexes parallel to and tilting to the radar beam respectively. Horizontal wind vectors and Doppler velocity fields adopted from Desrochers and Harris (1996).

well with each other but the location of the centers did not correspond well. The area of vortex obtained by the present automated method better represents the region of a large shear when compared to the area obtained by the Rankine vortex. We can consider that the values obtained by the present automated method are effective for practical use.

6. Summary

We devised the technique to detect vortexes automatically from the gradient of Doppler velocity data obtained from a single Doppler radar. In the application of the method, both SRD (Shear of Range Direction) and SAD (Shear of Azimuthal Direction) showed patterns that indicated a vortex. We confirmed that an anticyclonic or cyclonic vortex can be detected by a symmetric vortex pattern in the Doppler velocity field when the vortex is close to circular. Since we applied a method of gust front (shear line) detection to this technique, we could detect both gust fronts (shear line) and vortexes at the same time. We compared the diameters of cyclonic vortex patterns estimated by the assumptions of the Rankine vortex, with those obtained by the present automated method, and these coincided well each other.

Acknowledgments

The authors would like to express their thanks to Professor Katsuhiro Kikuchi for his encouragement throughout this work. Further, the authors would like to show their thanks to the students of the Meteorological Laboratory, Graduate School of Science, Hokkaido University, for their support of this work. One of the authors, Haneda is grateful to the parties concerned at Japan Radio Co., Ltd., for support of this work.

References

Desrochers, P.R. and F.I. Harris, 1996. Interpretation of mesocyclone vorticity and divergence structure from single-Doppler radar. J. Appl. Meteor., **35**, 2191-2209.

Haneda, T. and H. Uyeda, 1997. A technique for detecting a vortex using gradient of Doppler velocity data. Preprint Vol. 28th Int'l. Conf. on Radar Meteorology. Austin, 345-346.

Kobayashi, F., K. Kikuchi and H. Uyeda, 1996. Life cycle of the Chitose tornado of September 22, 1988. J. Meteor. Soc. Japan, **74**, 125-140.

Shirooka, R. and H. Uyeda, 1991. Doppler radar observation of tornado and microburst around Chitose airport. Preprint Vol. 25th Int'l. Conf. on Radar Meteorology. Paris, J73-J76.

Takahashi, N., H. Uyeda, K. Kikuchi and M. Okazaki, 1991. A method to describe the fluctuation and discontinuity of horizontal wind fields by a single Doppler radar. Preprint Vol. 25th Int'l. Conf. on Radar Meteorology. Paris, 642-645.

Uyeda, H. and D.S. Zrnic', 1986. Automatic detection of gust fronts. J. Atmos. Oceanic Technol., **3**, 36-50.

Uyeda, H. and D.S. Zrnic', 1988. Fine structure of gust fronts obtained from the analysis of single Doppler radar data. J. Meteor. Soc. Japan, **66**, 869-881.

Wood, V.T., and R.A. Brown, 1983. Single Doppler velocity signatures: An atlas of patterns in clear air/widespread precipitation and convective storms. NOAA Tech. Memo. ERL NSSL-95, 71pp.

Wood, V.T., 1994. A technique for detecting a tropical cyclone center using a Doppler radar. J. Atmos. Oceanic Technol., **11**, 1207-1216.

Zrnic', D.S., D.W. Burgess and L.D. Hennington, 1984. Automatic detection of mesocyclonic shear. J. Atmos. Oceanic Technol., **2**, 425-438.